ARTICLE
Journal of Cellular Biochemistry 107:240–252 (2009)

Journal of Cellular Biochemistry

Global Transcriptome Analysis in Mouse Calvarial Osteoblasts Highlights Sets of Genes Regulated by Modeled Microgravity and Identifies A "Mechanoresponsive Osteoblast Gene Signature"

Mattia Capulli, Anna Rufo, Anna Teti,* and Nadia Rucci

Department of Experimental Medicine, University of L'Aquila, L'Aquila, Italy

ABSTRACT

Mechanical unloading is known to be detrimental for the skeleton, but the underlying molecular mechanisms are not fully elucidated. We performed global transcriptome analysis of mouse calvarial osteoblasts grown for 5 days at unit gravity (1*g*) or under modeled microgravity (0.008*g*) in the NASA-developed rotating wall vessel (RWV) bioreactor. Elaboration of gene profiling data evidenced that, among the >20,000 gene probes evaluated, 45 genes were significantly up-regulated (cut-off >2) and 88 were down-regulated (cut-off <0.5) in modeled microgravity versus 1*g*. This set of regulated genes includes genes involved in osteoblast differentiation, function, and osteoblast–osteoclast cross-talk, as well as new genes not previously correlated with bone metabolism. Microarray data were validated for subsets of genes by real-time RT-PCR, Western blot, or functional analysis. The significantly modulated genes were then clustered using the GOTM (Gene Ontology Tree Machine) software. This analysis evidenced up-regulation of genes involved in the induction of apoptosis, in response to stress and in the activity of selected growth factors. Other molecular functions, such as extracellular matrix structural constituent, glycosaminoglycan/heparin-binding activity, and other growth factor activity, were instead down-regulated. We finally matched our transcriptome results with other public global gene profiles obtained in loading and unloading conditions, identifying 10 shared regulated genes which could represent an "osteoblast mechanoresponsive gene signature." J. Cell. Biochem. 107:240–252, 2009.

KEY WORDS: MODELED MICROGRAVITY; OSTEOBLAST; GENE PROFILING; UNLOADING

Recent biomedical studies have provided compelling evidence that weightlessness induces several pathological conditions in astronauts, including immune dysfunctions [Sonnenfeld et al., 2003], cardiovascular problems [Tuday et al., 2007], muscle atrophy [Tesch et al., 2005], and skeletal alterations eventually leading to a decrease of bone mass and bone demineralization [Van Loon et al., 1995; Collet et al., 1997; Carmeliet and Bouillon, 1999; Caillot-Augusseau et al., 1998, 2000]. Indeed, it has been estimated that 1–2% site-specific bone loss occurs in the human skeleton each month during spaceflight [Tilton et al., 1980], and the severity of this phenomenon directly correlates with flight duration [Bikle and Halloran, 1999].

Development of this pathological condition is consistent with the notion that mechanical loading is critical for the maintenance of a balanced bone mass, as also demonstrated by the evidence that other unloading conditions, such as bed rest immobilization, motor paralyses, and reduced physical activity with aging cause bone loss, eventually leading to osteoporosis [Robling et al., 2001].

Bone remodeling is an active and dynamic process which requires that osteoblasts, the cells with osteogenic function, and osteoclasts, the cells resorbing bone, work in concert to maintain a constant bone mass. Indeed, bone tissue responds to mechanical loading by activation of bone formation and inhibition of bone resorption [Hsieh et al., 2001].

Based on this evidence, it is conceivable that bone loss observed under weightlessness could be explained by a reduction of osteoblast function and/or by an increased osteoclast bone resorption. Indeed, several human studies during spaceflights showed decreased serum levels of bone formation markers, including alkaline phosphatase (ALP), osteocalcin (OCN), and the C-terminal peptide of pro-collagen I [Collet et al., 1997; Caillot-Augusseau et al., 2000]. Ground-based studies performed using

Mattia Capulli and Anna Rufo contributed equally to this work.

Grant sponsor: Agenzia Spaziale Italiana (ASI); Grant number: I/007/06/0.

*Correspondence to: Prof. Anna Teti, PhD, Department of Experimental Medicine, Via Vetoio, Coppito 2, 67100 L'Aquila, Italy. E-mail: teti@univaq.it

Received 29 October 2008; Accepted 4 February 2009 • DOI 10.1002/jcb.22120 • 2009 Wiley-Liss, Inc.
Published online 13 March 2009 in Wiley InterScience (www.interscience.wiley.com).

different models of simulated microgravity confirmed bone formation defects [Nakamura et al., 2003; Zayzafoon et al., 2004; Pardo et al., 2005].

Although these studies have helped to explain, at least in part, the bone loss due to weightlessness, the underlying cellular and molecular mechanisms are not at all elucidated. To more deeply dissect these mechanisms, we performed whole genome microarray analysis on primary osteoblasts grown at unit gravity or under simulated microgravity using the NASA-developed rotary cell culture system (RCCS) equipped with a rotating wall vessel (RWV) bioreactor [Duray et al., 1997; Rucci et al., 2002, 2007; Patel et al., 2007]. We identified a subset of genes significantly regulated by microgravity, some of which obviously correlated with osteoblast differentiation and function, while for others no correlation had been found so far with bone metabolism. These latter could represent new osteoblast determinants regulating bone mass.

MATERIALS AND METHODS

MATERIALS

Dulbecco's-modified minimum essential medium (DMEM), fetal bovine serum (FBS), penicillin, streptomycin, and trypsin were from Invitrogen (Carlsbad, CA). Sterile plastic ware was from Falcon Becton–Dickinson (Cowley, Oxford, UK) or Costar (Cambridge, MA). CultiSpher-G® microcarriers (#D-G0001-OO) were from Percell Biolytica AB (Astorp, Sweden). Kits for preparation and hybridization of samples and microarray chips were from Agilent Technologies, Inc. (Santa Clara, CA). The Trizol reagent, primers, and reagents for RT-PCR were from Invitrogen. The Brilliant® SYBR® Green QPCR master mix was from Stratagene (La Jolla, CA). Enhanced ChemiLuminescence (ECL) kit and Hybond nitrocellulose were from Amersham Pharmacia Biotech (Little Chalfont, Bucks, UK). Anti-Mimecan (#AF2949), anti-Lipocalin 2/NGAL antibodies (#AF1857), and donkey anti-goat IgG HRP-conjugated antibody (#HAF109) were from R&D systems (Minneapolis, MN). Anti-cadherin 11 antibody (#sc-28643) and goat anti-rabbit IgG HRP-conjugated antibody (#sc-2004) were from Santa Cruz Biotechnology, Inc. (Heidelberg, Germany). ELISA kit for mouse soluble RANK-L (receptor activator of NF-kappaB) (#MTR00), osteoprotegerin (OPG) (#MOP00), and mouse interleukin-6 (IL-6) (#M6000B) were from R&D systems. All other reagents were from Sigma–Aldrich Co. (St. Louis, MO).

ROTATING WALL VESSEL (RWV) BIOREACTOR

The RWV Bioreactor (model STLV, size 55 ml; Synthecon CELLON S.ar.l, Strassen, Luxembourg) is a horizontal rotating, bubble-free culture vessel with membrane diffusion gas exchange, where the culture medium and the cells on microcarriers rotate inside the vessel with very low fluid stress forces [Duray et al., 1997; Rucci et al., 2002, 2007; Patel et al., 2007]. Microcarriers are in suspension and rotate inside the vessel of the bioreactor as a solid body. Moreover, the horizontal rotation of the vessel subjects the cells to a constant randomization of the normal gravity vector, thus mimicking a state of simulated free fall. The use of microcarrier beads is strongly suggested by the manual of the RWV bioreactor especially for cultures of adhesive cells, such as the osteoblasts.

PRIMARY OSTEOBLAST CULTURES

Calvariae from 7-days-old CD1 mice were removed and processed as previously described [Marzia et al., 2000]. The harvested cells, cultured in a static 2D culture system (adhesive flasks) expressed the osteoblast markers ALP, Runx2, parathyroid hormone/parathyroid hormone-related peptide receptor, type I collagen, and OCN.

At confluence, cells were collected and resuspended in DMEM + 10% FBS containing CultiSpher-G® microcarriers (1 g/L medium), at a cellular density of 1.2×10^6 cells/ml, to allow cell–microcarrier interaction. This suspension was then grown for 5 days into the RWV bioreactor under a 16-rpm rotation, which leads to a simulated microgravity condition of 0.008*g*, or in non-adhesive Petri dishes, that is the unit gravity condition (1*g*). For some experiments, cells were also subjected to a rotation of 50 rpm, leading to a simulated microgravity of 0.08*g*, or were subjected to a simulated microgravity condition of 0.008*g* for 1, 3, and 5 days. At the end of the experiments, cells were collected and subjected to RNA or protein extraction.

cDNA MICROARRAY ASSAY

Total RNA from osteoblasts cultured at unit gravity or at 0.008*g* gravity was extracted using TRIzol procedure following the manufacturer's instructions. RNA integrity was assessed by agarose gel electrophoresis. The RNA was then quantified by absorbance at 260 nm and its purity checked by evaluation of 260/280 nm ratio.

cDNAs were obtained employing the fluorescent direct label kit from Agilent®. Briefly, 20 μg of RNA was retro-transcribed in the presence of the cyanine 3-dCTP (cy3-dCTP) or the cyanine 5-dCTP (cy5-dCTP) and hybridized with the 22K oligo-microarray (Agilent's Mouse Oligo Microarray). The microarray slides were then scanned using the Affymetrix® microarray scanner, Mod. 428.

Microarray analysis was performed for three experiments, each run in duplicate in order to invert the cy3 and cy5 labeling.

MICROARRAY DATA ANALYSIS

Arrays data were analyzed by the following dedicated software:

Jaguar Software® version 2.0 (Affymetrix) for the acquisition of the microarray image, scanning the cy3 and cy5 fluorescence.
ImaGene® Software (BioDiscovery, Inc.) to quantify the fluorescence intensities of each spot.
VectorXpression® Version 4.1 (Invitrogen) to fully analyze the microarray data.

Each array was normalized by shifting the global minimum value to 0 to reduce the differences in fluorescence intensity in different arrays. The gene profiles from each microarray were then normalized versus a set of 10 house-keeping genes [Kouadjo et al., 2007], including *beta-actin* and *gapdh*, and genes were filtered using two parameters: statistical significance (*P*-value, obtained from a *t*-test performed on all the arrays, <0.05) and functional significance (ratio value, obtained from the ratio of the 0.008*g* value vs. unit gravity value, with a cut-off >2 or <0.5).

Finally, the significantly regulated genes were clustered using a web-based platform GOTM (Gene Ontology Tree Machine) [Zhang et al., 2004]. The software uses statistical analysis indicating GO

terms with relatively enriched gene numbers and suggesting interesting biological areas.

REAL-TIME RT-PCR

Total RNA was extracted using the TRIzol procedure. Two micrograms of RNA was reverse-transcribed using Moloney murine leukemia virus reverse transcriptase, and the equivalent of 0.1 μg was used for PCR reactions. Real-time PCR was performed employing the Brilliant SYBR Green QPCR master mix using conditions and primer pairs listed in Table I.

WESTERN BLOTTING

For total protein extraction, cells were lysed in RIPA buffer (50 mM Tris–HCl, pH 7.5, 150 mM NaCl, 1% Nonidet P-40, 0.5% sodium deoxycholate, 0.1% SDS) containing protease inhibitors. Proteins were resolved by 10% SDS–PAGE and transferred to nitrocellulose membranes. Blots were probed with the primary antibody for 1 h at room temperature, washed and incubated with the appropriate HRP-conjugated secondary antibody for 1 h at room temperature. Protein bands were revealed by ECL.

ELISA ASSAYS

Soluble RANKL, OPG, and IL-6 were quantified in conditioned media using the R&D System ELISA kits #MTR00, #MOP00, and #M6000B, respectively, according to the manufacturer's instructions.

PROLIFERATION ASSAY

Calvarial osteoblasts (10,000/well) were cultured in 24-well plates in the presence of vehicle (acetic acid 10 mM) or of 5 ng/ml recombinant human IL-6 (rhIL-6). Twenty-four hours later, medium was replaced with DMEM plus 1% FBS and, after 24 h, 2 μCi/ml ^{3}H-thymidine (specific activity 25 Ci/mmol) was added to each well and incubated overnight. After 24 h, cells were lysed in 0.1% SDS, precipitated in 100% TCA, and the incorporated ^{3}H-thymidine was measured in a beta counter.

ALKALINE PHOSPHATASE (ALP) ACTIVITY

Calvarial osteoblasts were treated for 5 days with vehicle or with 5 ng/ml of rhIL-6. Cells were then fixed in 4% paraformaldehyde in 0.1 M cacodylate buffer for 15 min and washed with the same buffer. ALP activity was evaluated histochemically using reagents and protocol from Sigma–Aldrich, kit no. 104-LS.

MINERALIZATION ASSAY

For mineralization assay, standard medium was supplemented with 10 mM β-glycerophosphate and 50 μg/ml of ascorbic acid, and calvarial osteoblasts were cultured with or without 5 ng/ml of rhIL-6 for 3 weeks, then detection of mineralization was performed by the von Kossa staining.

STATISTICS

All experiments were repeated at least three times. Data are expressed as the mean ± SEM. Statistical analysis was performed by one-way analysis of variance, followed by unpaired Student's *t*-test. A *P*-value <0.05 was conventionally considered statistically significant.

RESULTS

GENE EXPRESSION PROFILE OF OSTEOBLASTS UNDER MODELED MICROGRAVITY

In our culture condition, osteoblasts grew on the microcarrier surface and within their pores, interacting each other and with the microcarrier surface to which they adhered (Fig. 1A). Large-scale microarray analysis was performed on these osteoblasts subjected for 5 days to 1*g* or to 0.008*g* (modeled microgravity), using the Agilent's Mouse Oligo Microarray, which contained 22,575 oligonucleotide probes representing over 20,000 well-characterized mouse transcripts. Figure 1B shows the scatter plot obtained after the analysis of three experiments. Our final elaboration, using a cut-off <0.5 and >2 and a statistical significance of $P < 0.05$, evidenced N. 88 genes down-regulated and N. 45 genes up-regulated, listed in Table II.

mRNA AND PROTEIN VALIDATION OF THE MICROGRAVITY OSTEOBLAST GENES

To validate our gene profiling results, comparative real-time RT-PCR and Western blot analysis were performed for a selected subset of genes. For RT-PCR genes were selected randomly, while for

TABLE I. Primer Pairs Employed for Real-Time RT-PCR

	Primers	
Gene	Forward	Reverse
Gapdh	5′-TGGCAAAGTGGAGATTGTTGC -3′	5′-AAGATGGTGATGGGCTTCCCG-3′
Runx2	5′-AACCCACGGCCCTCCCTGAACTCT-3′	5′-ACTGGCGGGGTGTAGGTAAAGGTG-3′
IL-6	5′-GAGGATACCACTCCCAACAGACC-3′	5′-AAGTGCATCATCGTTGTTCATACA-3′
Rankl	5′-CCAAGATCTCTAACATGACG-3′	5′-CACCATCAGCTGAAGATAGT-3′
Penk 1	5′-GACAGCAGCAAACAGGATGA-3′	5′-GTTGTCTCCCGTTCCCAGTA-3′
Aspn	5′-AGGACACGTTCAAGGGAATG-3′	5′-AGGCCTTTTGGAATTGAGGT-3′
Ogn	5′-TGCAACAGGCAATTCTGAAG-3′	5′-TCCTTGGCAGTCAGCTTTTT-3′
Cdh11	5′-TCGCAGCAGAAATTCACAAC-3′	5′-CTCCACGTCGGGCATATACT-3′
Nqo 1	5′-TTCTCTGGCCGATTCAGAGT-3′	5′-GGCTGCTTGGAGCAAAATAG-3′
Lcn 2	5′-CCAGTTCGCCATGGTATTTT-3′	5′-CACACTCACCACCCATTCAG-3′
Tnmd	5′-AGAATGAGCAATGGGTGGTC-3′	5′-CTCGACCTCCTTGGTAGCAG-3′
Opg	5′-AAAGCACCCTGTAGAAAACA-3′	5′-CCGTTTTATCCTCTCTACACTC-3′

PCR conditions were 40 cycles: 94°C for 45 s, 60°C for 45 s, and 72°C for 45 s.

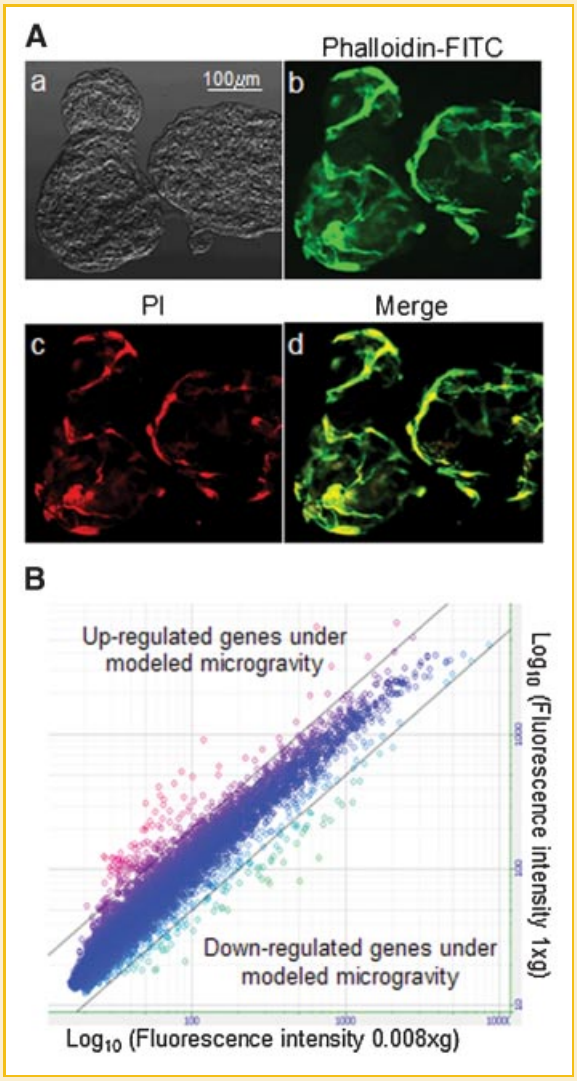

Fig. 1. A: Primary osteoblasts cultured on microcarriers in the RWV bioreactor. Primary osteoblasts were obtained from calvariae of 7 days old mice. At confluence, cells were collected in DMEM + 10% FBS containing CultiSpher-G® microcarriers (1 g/L medium), at a cellular density 1.2×10^6 cells/ml and grown into the RWV bioreactor under a 16 rpm rotation (0.008*g*). After 5 days, microcarriers were collected, attached to glass slides by cytospin procedure, fixed, and stained with fluorescein thiocyanate (FITC)-conjugated phalloidin to mark the actin microfilaments (green), and with propidium iodide (PI) (red) to mark the nuclei. a: Phase contrast microscopy showing a microcarrier loaded with the osteoblasts. b,c: Confocal microscopy of the same microcarrier showing (b) osteoblast cytoskeleton and (c) nuclei. In (d) merged picture of the two fluorescences (b,c) is shown. B: Effect of modeled microgravity on osteoblast gene expression profile. Primary osteoblasts grown for 5 days at unit gravity (1*g*) or in the RWV under modeled microgravity (0.008*g*) as described in (A) were collected and the RNA extracted, reverse-transcribed, and labeled with cy3-dCTP and cy5-dCTP fluorochromes. Labeled probes were hybridized onto 22K mouse oligomicroarray (Agilent®). Slides were then scanned in an Affymetrix® microarray scanner (mod. 428) using the ImaGene® software. The scatter plot shows mean intensities of each gene probes obtained from three independent experiments, each run in duplicate. Lines represent two standardized cut off, the genes above the upper line are up-regulated by modeled microgravity, the genes below the lower line are down-regulated, and genes falling between the two lines are iso-expressed in the two conditions.

Western blot we selected a group of proteins whose antibodies were commercially available. We confirmed a decrease in *Cadherin 11* (*Cdh11*) (Fig. 2A) and *Osteoglycin* (*Ogn*) (Fig. 2B) mRNAs and an increase of *Lipocalin 2* (*Lcn2*) (Fig. 2C), the latter being the most up-regulated gene (Table II). Consistently, similar pattern of regulation was found at the protein level (Fig. 2D–F). Modulation of other genes, such as *Asporin* (*Aspn*) (Fig. 3A), *NAD(P)H dehydrogenase quinone 1* (*Nqo1*) (Fig. 3B), *Tenomodulin* (*Tnmd*) (Fig. 3C), and the most down-regulated gene *Preproenkephalin 1* (*Penk1*) (Fig. 3D) was also confirmed by real-time RT-PCR.

All genes selected for validation were confirmed to be regulated in concordance with the microarray analysis. Altogether, these results provide compelling evidence of the reliability of our gene profiling results.

RELATIONSHIP BETWEEN GENE REGULATION AND INTENSITY OF GRAVITATIONAL FORCE

In order to assess whether the degree of gene regulation was dependent on intensity of gravitational force, selected genes were analyzed by real-time RT-PCR in osteoblasts subjected to 1, 0.08, and 0.008*g*. As expected, results demonstrated "gravitational force-dependent" regulation for all genes tested, which included *Tnmd*, *Aspn*, *IL-6* (not shown), *Lcn2* (Fig. 3E), *Nqo1* (Fig. 3F), *Cdh11* (Fig. 3G), and *Penk1* (Fig. 3H).

RELATIONSHIP BETWEEN GENE REGULATION AND DURATION OF SIMULATED MICROGRAVITY

We also investigated the time-dependent effect of simulated microgravity on gene regulation. Osteoblasts were maintained under 1 or 0.008*g* for 1, 3, or 5 days, then mRNA expression of the most up- and down-regulated genes were assessed by real-time RT-PCR. Figure 4 shows that all genes analyzed had a time-dependent pattern of regulation. *Lcn2*, *IL-6*, and *Nqo1* progressively increased up to 5 days of microgravity. Similarly, *Penk1* progressively decreased and achieved maximal down-regulation at 5 days, while *Asp* showed maximal reduction at 1 day and *Tnmd* at 3 days of microgravity.

EVALUATION OF THE REGULATED GENES ASSOCIATED WITH OSTEOBLAST DIFFERENTIATION AND FUNCTION

We next identified single genes potentially relevant for bone loss induced by unloading conditions. Indeed, among the significantly down-regulated genes we recognized *Sfrp2* (*Secreted frizzled related sequence protein 2*) and *Wisp2* (*WNT1 inducible signaling pathway protein 2*) (Table II) which are involved in the Wnt pathway, thus concurring to osteoblast differentiation, whose reduction was validated by real-time RT-PCR analysis (Fig. 5A,B). As far as the master gene *Runx2* (*Runt-related transcription factor 2*) is concerned, we found that it was down-regulated with a value and a significance very close to the cut-off applied (Fig. 5C, inset table). This regulation was significant in real-time RT-PCR analysis (Fig. 5C, graph).

We also assessed the regulation of genes involved in osteoblast–osteoclast cross-talk, such as *RankL* (*Receptor Activator of NF-kappaB Ligand*) and its decoy receptor *OPG*. In agreement with our previous results obtained after 24 h of modeled microgravity [Rucci

TABLE II. List of the Significantly Regulated Genes Under Modeled Microgravity

Systematic name	Gene symbol	Gene name	Fold Δ	*P*-value
Down-regulated genes (cut-off <0.5; $P < 0.05$)				
NM_001002927	Penk1	Preproenkephalin 1	0.09506	0.00003
NM_025711	Aspn	Asporin	0.15440	0.02117
NM_022322	Tnmd	Tenomodulin	0.17625	0.00077
NM_029803	Ifi27	Interferon, alpha-inducible protein 27	0.19802	0.01181
NM_030707	Msr2	Macrophage scavenger receptor 2	0.19816	0.00684
NM_008760	Ogn	Osteoglycin	0.20683	0.01163
NM_009144	Sfrp2	Secreted frizzled-related sequence protein 2	0.20936	0.00891
NM_011313	S100a6	S100 calcium-binding protein A6 (calcyclin)	0.21673	0.03344
AK003938	Fndc1	Fibronectin type III domain containing 1	0.22215	0.00072
NM_054098	Steap4	STEAP family member 4	0.22440	0.00007
NM_007739	Col8a1	Procollagen, type VIII, alpha 1	0.24583	0.00025
NM_011331	Ccl12	Chemokine (C-C motif) ligand 12	0.24945	0.00431
AK018112	9930013L23Rik	RIKEN cDNA 9930013L23 gene	0.26844	0.01372
NM_008625	Mrc1	Mannose receptor, C type 1	0.26947	0.01416
NM_026516	2810417M05Rik	RIKEN cDNA 2810417M05 gene	0.27101	0.00466
NM_008278	Hpgd	Hydroxyprostaglandin dehydrogenase 15 (NAD)	0.27437	0.00089
XM_619396	D930038M13Rik	RIKEN cDNA D930038M13 gene	0.27774	0.00065
NM_010217	Ctgf	Connective tissue growth factor	0.28212	0.02596
NM_021472	Rnase4	Ribonuclease, RNase A family 4	0.30053	0.00149
NM_024283	1500015O10Rik	RIKEN cDNA 1500015O10 gene	0.31031	0.00366
X56397	Vim	Vimentin	0.32531	0.02698
NM_023386	5830458K16Rik	RIKEN cDNA 5830458K16 gene	0.33645	0.00128
NM_146015	Efemp1	Epidermal growth factor-containing fibulin-like extracellular matrix protein 1	0.33876	0.00058
NM_009155	Sepp1	Selenoprotein P, plasma, 1	0.33995	0.0102
AK047014	Itgbl1	Integrin, beta-like 1	0.34185	0.0017
NM_008590	Mest	Mesoderm-specific transcript	0.34622	0.00276
XM_485004	LOC433432	Similar to rbm3	0.35097	0.0002
NM_010233	Fn1	Fibronectin 1	0.35479	0.02092
NM_009606	Acta1	Actin, alpha 1, skeletal muscle	0.35498	0.01583
NM_012050	Omd	Osteomodulin	0.35951	0.02716
NM_009608	Actc1	Actin, alpha, cardiac	0.36009	0.00895
NM_009721	Atp1b1	ATPase, Na+/K+ transporting, beta 1 polypeptide	0.36383	0.00332
NM_181277	Col14a1	Procollagen, type XIV, alpha 1	0.36716	0.00759
AK003142	H19	H19 fetal liver mRNA	0.36979	0.02231
NM_008809	Pdgfrb	Platelet-derived growth factor receptor, beta polypeptide	0.37346	0.02980
NM_008409	Itm2a	Integral membrane protein 2A	0.37458	0.00528
NM_009866	Cdh11	Cadherin 11	0.37530	0.02392
NM_008538	Marcks	Myristoylated alanine-rich protein kinase C substrate	0.37593	0.01327
NM_007654	Cd72	CD72 antigen	0.37661	0.00829
NM_015784	Postn	Periostin, osteoblast-specific factor	0.37931	0.00759
NM_133775	9230117N10Rik	RIKEN cDNA 9230117N10 gene	0.38372	0.03228
NM_010160	Cugbp2	CUG triplet repeat, RNA-binding protein 2	0.38408	0.02226
NM_008987	Ptx3	Pentraxin-related gene	0.38426	0.04775
NM_017372	Lyzs	Lysozyme	0.38847	0.08561
NM_010917	Nid1	Nidogen 1	0.39442	0.00441
NM_010514	Igf2	Insulin-like growth factor 2	0.39780	0.00506
NM_009365	Tgfb1i1	Transforming growth factor beta 1-induced transcript 1	0.40112	0.01957
NM_016911	Srpx	Sushi-repeat-containing protein	0.40409	0.02429
NM_010195	Lgr5	Leucine-rich repeat containing G protein coupled receptor 5	0.40439	0.04490
NM_011415	Snai2	Snail homolog 2 (Drosophila)	0.40656	0.00165
NM_011653	Tuba1	Tubulin, alpha 1	0.40787	0.00278
NM_009131	Clec11a	C-type lectin domain family 11, member a	0.40896	0.01014
NM_016873	Wisp2	WNT1 inducible signaling pathway protein 2	0.41753	0.04994
NM_031185	Akap12	A kinase (PRKA) anchor protein (gravin) 12	0.42647	0.00716
NM_025569	Mgst3	Microsomal glutathione S-transferase 3	0.42784	0.00682
D13903	Ptprd	Protein tyrosine phosphatase, receptor type, D	0.42839	0.01666
AI386420	Ifitm6	Interferon-induced transmembrane protein 6	0.43144	0.03323
NM_177715	Kctd12	Potassium channel tetramerization domain containing 12	0.44228	0.00097
NM_008546	Mfap2	Microfibrillar-associated protein 2	0.44903	0.02579
NM_148933	Slco4a1	Solute carrier organic anion transporter family, member 4a1	0.45125	0.01714
NM_008242	Foxd1	Forkhead box D1	0.45493	0.01513
BC030317	Lrrc17	Leucine-rich repeat containing 17	0.45605	0.01359
NM_007584	Ddr1	Discoidin domain receptor family, member 1	0.45836	0.02722
NM_021274	Cxcl10	Chemokine (C-X-C motif) ligand 10	0.45867	0.02961
NM_021278	Tmsb4x	Thymosin, beta 4, X chromosome	0.46076	0.00306
AK028745	2310043N10Rik	RIKEN cDNA 2310043N10 gene	0.46147	0.00949
AK046712	B430320C24Rik	RIKEN cDNA B430320C24 gene	0.46481	0.01557
AK028562	Plxna2	Plexin A2	0.46725	0.01677
NM_009128	Scd2	Stearoyl-coenzyme A desaturase 2	0.46924	0.00671
NM_007393	Actb	Actin, beta, cytoplasmic	0.47006	0.04109
NM_008087	Gas2	Growth arrest specific 2	0.47436	0.00193
NM_007792	Csrp2	Cysteine and glycine-rich protein 2	0.47638	0.02587
NM_173375	BC064033	cDNA sequence BC064033	0.47667	0.02437
NM_026142	3632451O06Rik	RIKEN cDNA 3632451O06 gene	0.47978	0.00033
AK019479	Unknown	Unknown	0.48479	0.01173
NM_026082	Dock7	Dedicator of cytokinesis 7	0.48491	0.03013

TABLE II. (*Continued*)

Systematic name	Gene symbol	Gene name	Fold Δ	*P*-value
NM_016904	Cks1b	CDC28 protein kinase 1b	0.48493	0.01694
NM_178660	Rbms3	RNA-binding motif, single-stranded interacting protein	0.48529	0.02274
NM_008968	Ptgis	Prostaglandin I2 (prostacyclin) synthase	0.48546	0.01342
XM_485171	Myl9	Myosin, light polypeptide 9, regulatory	0.48661	0.04406
NM_011821	Gpc6	Glypican 6	0.48972	0.04259
AF020194	Slc6a6	Solute carrier family 6 (neurotransmitter transporter, taurine), member 6	0.49083	0.00360
AK003303	Ptprd	Protein tyrosine phosphatase, receptor type D	0.49094	0.02306
NM_026517	Rpl22l1	Ribosomal protein L22 like 1	0.49411	0.00043
NM_130449	Colec12	Collectin sub-family member 12	0.49506	0.00898
NM_023672	Ssbp3	Single-stranded DNA-binding protein 3	0.49658	0.00891
NM_023119	Eno1	Enolase 1, alpha non-neuron	0.49680	0.01017
NM_029568	Mfap4	Microfibrillar-associated protein 4	0.49693	0.00809
Up-regulated genes (cut-off >0.5; $P < 0.05$)				
NM_008491	Lcn2	Lipocalin 2	8.53243	0.01036
NM_008706	Nqo1	NAD(P)H dehydrogenase, quinone 1	6.38540	0.00543
XM_355243	Prg4	Proteoglycan 4 (megakaryocyte-stimulating factor, articular superficial zone protein)	5.04177	0.01438
NM_031168	Il6	Interleukin 6	4.44137	0.04785
NM_007695	Chi3l1	Chitinase 3-like 1	3.76403	0.00084
NM_016903	Esd	Esterase D/formylglutathione hydrolase	3.55810	0.00082
NM_010809	Mmp3	Matrix metalloproteinase 3	3.33807	0.04335
NM_015762	Txnrd1	Thioredoxin reductase 1	3.30237	0.00371
AV030849	Unknown	Unknown	3.22485	0.00154
NM_011593	Timp1	Tissue inhibitor of metalloproteinase 1	2.96405	0.00047
NM_011171	Procr	Protein C receptor, endothelial	2.80662	0.04165
NM_144923	Blvrb	Biliverdin reductase B (flavin reductase (NADPH))	2.70638	0.01320
NM_011315	Saa3	Serum amyloid A 3	2.70421	0.02030
NM_010442	Hmox1	Heme oxygenase (decycling) 1	2.66387	0.00384
NM_013671	Sod2	Superoxide dismutase 2, mitochondrial	2.65355	0.00220
NM_008380	Inhba	Inhibin beta-A	2.52867	0.00066
NM_013609	Ngfb	Nerve growth factor, beta	2.51409	0.03235
ENSMUST0000007	Unknown	Unknown	2.46648	0.00196
NM_177256	Prdx6-rs1	Peroxiredoxin 6, related sequence 1	2.42005	0.00653
NM_025549	Arrdc4	Arrestin domain containing 4	2.41773	0.01723
NM_009285	Stc1	Stanniocalcin 1	2.39013	0.02904
AK035610	9530076L18	Hypothetical protein 9530076L18	2.34080	0.00410
NM_008303	Hspe1	Heat shock protein 1 (chaperonin 10)	2.32711	0.00456
NM_053153	Klra18	Killer cell lectin-like receptor, subfamily A, member 18	2.32509	0.01131
AK010095	2310067L16Rik	RIKEN cDNA 2310067L16 gene	2.29916	0.00419
NM_013559	Hsp105	Heat shock protein 105	2.28592	0.00033
NM_010479	Hspa1a	Heat shock protein 1A	2.25906	0.02453
NM_021507	Sqrdl	Sulfide quinone reductase-like (yeast)	2.24957	0.00081
NM_009344	Phlda1	Pleckstrin homology-like domain, family A, member 1	2.24096	0.04785
NM_175329	MGI:2143558	Nur77 downstream gene 2	2.23077	0.02353
NM_178917	Arrdc3	Arrestin domain containing 3	2.22372	0.03085
NM_007453	Prdx6	Peroxiredoxin 6	2.21996	0.00670
NM_008176	Cxcl1	Chemokine (C-X-C motif) ligand 1	2.20381	0.00044
NM_030099	9530053H05Rik	RIKEN cDNA 9530053H05 gene	2.19624	0.03043
NM_029688	Srxn1	Sulfiredoxin 1 homolog (*S. cerevisiae*)	2.18642	0.00296
NM_030250	D10Ertd438e	DNA segment, Chr 10, ERATO Doi 438, expressed	2.16374	0.02532
NM_007808	Cycs	Cytochrome c, somatic	2.10341	0.00009
NM_030704	Hspb8	Heat shock 27 kDa protein 8	2.10277	0.00176
NM_025444	Taf13	TAF13 RNA polymerase II, TATA box-binding protein (TBP)-associated factor	2.08694	0.05027
NM_011804	Creg1	Cellular repressor of E1A-stimulated genes 1	2.06985	0.00986
NM_011660	Txn1	Thioredoxin 1	2.06288	0.00719
NM_009372	Tgif	TG interacting factor	2.01856	0.01508
NM_026932	Ebna1bp2	EBNA1-binding protein 2	2.00769	0.03127
NM_030612	Nfkbiz	Nuclear factor of kappa light polypeptide gene enhancer in B-cells inhibitor, zeta	2.00768	0.02397
NM_013541	Gstp1	Glutathione S-transferase, pi 1	2.00359	0.00032

et al., 2007], the microarray data evidenced a significant, although <2, increase of *RankL* also in long-term (5 days) conditions (Fig. 6A, inset table), which was confirmed to a greater extent by real-time RT-PCR (Fig. 6A, graph). Microarray analysis also showed a trend of decrease of *Opg* (Fig. 6B, inset table), which achieved statistical significance in real-time RT-PCR analysis (Fig. 6B, graph). These modulations led to a significant increase of the *RankL*/*Opg* ratio under modeled microgravity (Fig. 6C). Moreover, ELISA analysis on osteoblast-conditioned media evidenced a strong increase of secreted RANK-L (Fig. 6D) and a parallel decrease of OPG (Fig. 6E), with a final robust increase of the RANKL/OPG ratio as well (Fig. 6F). Notably, these results confirm the transcriptome results also at the protein level.

As far as the 45 genes up-regulated in the transcriptome profile are concerned, we found *IL-6* (Table II). This cytokine is also involved in osteoblast–osteoclast cross-talk and has a dual role in bone tissue, as it stimulates osteoclastogenesis and impairs osteoblast differentiation. We first confirmed IL-6 regulation at mRNA and protein level by real-time RT-PCR (Fig. 7A) and ELISA test (Fig. 7B), respectively. Next, we functionally validated the IL-6 regulation by investigating its ability to affect osteoblast differentiation and function. To this aim, primary calvarial osteoblast

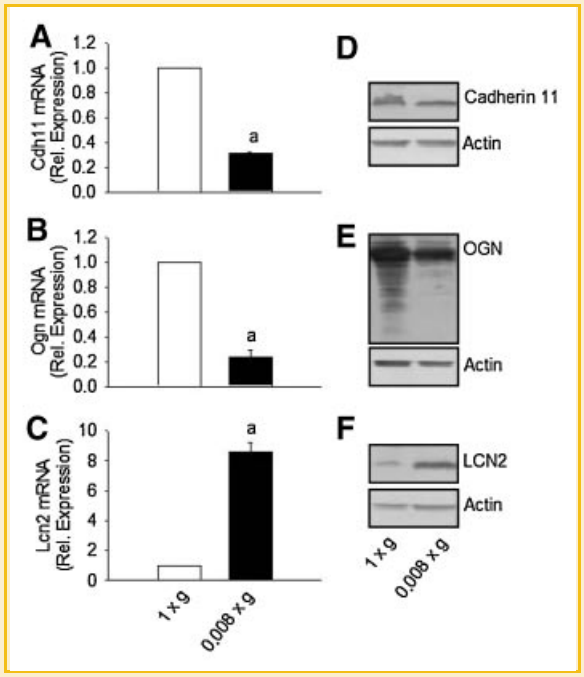

Fig. 2. Transcriptional and protein validation of microarray data. Primary osteoblasts were grown at unit gravity (1*g*) or under 0.008*g* modeled microgravity in the RWV bioreactor for 5 days, as described in Figure 1A. A–C: Cells were collected, the RNA extracted, and reverse-transcribed. cDNAs were subjected to comparative real-time PCR using primer pairs and conditions specific for (A) *Cadherin 11* (*Cdh11*), (B) *Osteoglycin* (*Ogn*), (C) *Lipocalin 2* (*Lcn2*). Data, normalized versus the house-keeping gene *Gapdh*, are the mean ± SEM of three independent experiments ($^{a}P < 0.01$ vs. 1*g*). D–F: Proteins were extracted and subjected to electrophoresis in a 10% SDS–PAGE. Filters were immunoblotted with (D) anti-CDH 11, (E) -OGN, (F) -LCN2 antibodies followed by incubation with specific HRP-conjugated secondary antibodies. Filters were then stripped and re-probed with anti-actin antibody for normalization. Results are representative of three independent experiments.

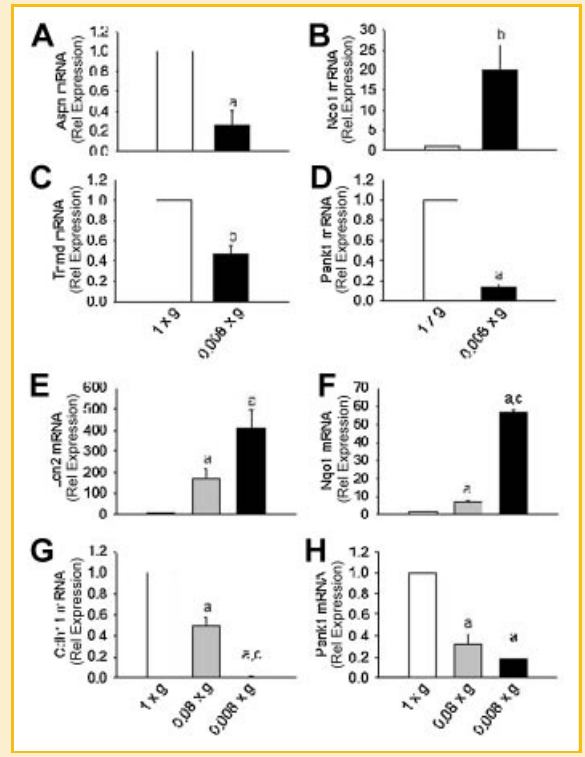

Fig. 3. Transcriptional validation and dependence on gravitational forces. Primary osteoblasts were grown at the indicated gravitational forces in the RWV bioreactor for 5 days as described in Figure 1A. Cells were collected, the RNA extracted, and reverse-transcribed. cDNAs were subjected to comparative real-time PCR using primer pairs and conditions specific for (A) *Asporin* (*Aspn*), (B,F) *NAD(P)H dehydrogenase quinone* 1 (*Nqo1*), (C) *Tenomodulin* (*Tnmd*), (D,H) *Preproenkephalin 1* (*Penk1*), (E) *Lipocalin 2* (*Lcn2*), and (G) *Cadherin 11* (*Cdh11*). Data, normalized versus the house-keeping gene *Gapdh*, are the mean ± SEM of three independent experiments ($^{a}P < 0.05$ vs. 1*g*; $^{b}P < 0.04$ vs. 1*g*; $^{c}P < 0.05$ vs. 0.08*g*).

cultures were treated with vehicle or hrIL6. In this circumstance, IL-6 treatment reduced proliferation (Fig. 7C) and differentiation of osteoblasts, the latter evidenced by a decrease of ALP activity (Fig. 7D). Interestingly, hrIL6 had similar effect on ALP activity even when the osteoblasts were cultured in the presence of β-glycerophosphate and ascorbic acid to enhance their differentiation (% of ALP positive cells vs. total cells: vehicle, 73 ± 2; hrIL-6, 45 ± 0.97, n = 3; $P = 0.0001$). Osteoblast function was also impaired, as demonstrated by reduced nodule mineralization (Fig. 7E).

GENE ONTOLOGY TERMS CLASSIFICATION OF THE DOWN-REGULATED GENES

Once identified to be significantly regulated by modeled microgravity, the genes were clustered according to the biological processes and the molecular functions in which they are involved in vivo, using the web-based platform GOTM [Zhang et al., 2004].

With regard to the down-regulated genes, we identified three molecular functions of interest that were impaired: extracellular matrix (ECM) components, glycosaminoglycan or heparin-binding activity and the activity of selected growth factors (Table III).

Among the genes whose products are ECM components and also bind glycosaminoglycans (Table III), there are *Osteomodulin* (*Omd*) and *Osteoglycin* (*Ogn*). These two proteoglycans belong to the small leucine rich-repeat proteoglycan (SLRP) family and are abundantly present in the bone matrix, cartilage cells, and connective tissues. *Omd* codes for a protein, also known as osteoadherin (OSAD), forming a bone proteoglycan containing keratan sulfate, specifically expressed in mineralized tissues [Sommarin et al., 1998] where it binds the osteoblasts via the αVβ3 integrin. Moreover, OSAD is involved in bone mineralization by cooperating with the bone sialoprotein [Ramstad et al., 2003; Rehn et al., 2006]. OGN, also known as mimecan and osteoinductive factor, is involved in the regulation of collagen fibrillogenesis [Tasheva et al., 2002] and is up-regulated during BMP-2-mediated osteoblast differentiation [Balint et al., 2003]. *Connective Tissue Growth Factor* (*Ctgf*), which is known to be induced by TGF-β1 and to favor osteoblast differentiation [Arnott et al., 2007], is also an ECM constituent and has glycosaminoglycan/heparin-binding activity. This gene was consistently down-regulated by modeled microgravity, as illustrated in Table II.

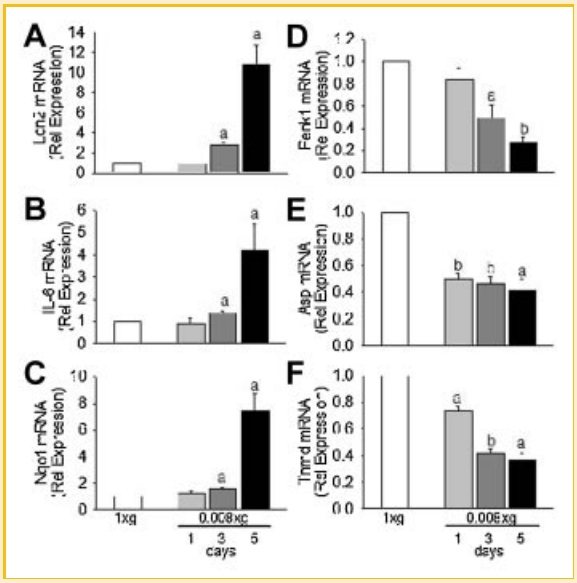

Fig. 4. Time-dependent regulation of gene expression. Primary osteoblasts were grown at unit gravity (1*g*) or under 0.008*g* modeled microgravity in the RWV bioreactor for 1, 3, or 5 days as described in Figure 1A. Cells were collected, the RNA extracted, and reverse-transcribed. cDNAs were subjected to comparative real-time PCR using primer pairs and conditions specific for (A) *Lipocalin 2* (*Lcn2*), (B) *Interleukin-6* (*IL-6*), (C) *NAD(P)H dehydrogenase quinone* 1 (*Nqo1*), (D) *Preproenkephalin 1* (*Penk1*), (E) *Asporin* (*Aspn*), and (F) *Tenomodulin* (*Tnmd*). Data, normalized versus the house-keeping gene *Gapdh*, are the mean ± SEM of three independent experiments ($^{a}P < 0.05$ and $^{b}P < 0.005$ vs. 1*g*).

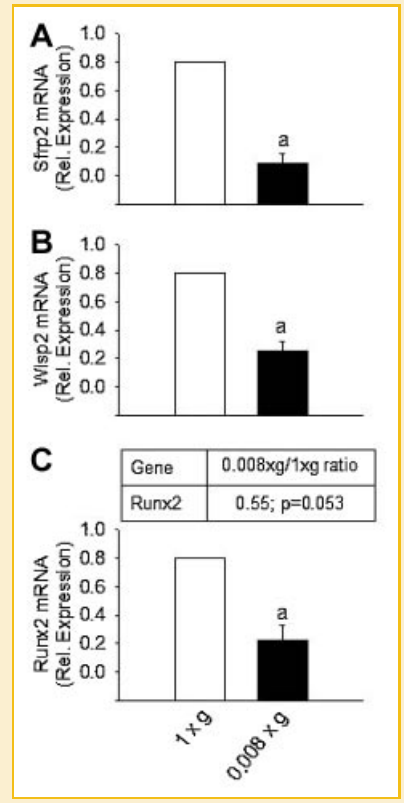

Fig. 5. Evaluation of the regulated genes associated with osteoblast differentiation and function. Primary osteoblasts were grown at unit gravity (1*g*) or under 0.008*g* modeled microgravity for 5 days as described in Figure 1A. Cells were collected, the RNA extracted, and reverse-transcribed. cDNAs were subjected to comparative real-time PCR using primer pairs and conditions specific for (A) *Secreted frizzled related sequence protein 2* (*Sfrp2*), (B) *WNT1 inducible signaling pathway protein 2* (*Wisp2*), and (C) *Runt-related transcription factor 2* (*Runx2*). Inset table in (C) shows the 0.008/1*g* ratio and *P*-value for the indicated gene obtained by microarray analysis. Data, normalized versus the house-keeping gene *Gapdh*, are the mean ± SEM of three independent experiments ($^{a}P < 0.05$ vs. 1*g*).

As far as the glycosaminoglycans/heparin-binding molecular function is concerned (Table III), we also found *Periostin* (*Pstn*) and *Fibronectin 1* (*Fn1*). *Pstn* encodes for a secreted protein highly expressed in early osteoblasts, which plays a role in the recruitment and attachment of osteoblast precursors to the periosteum [Horiuchi et al., 1999] while *Fn1* is a glycoprotein of the bone ECM involved in osteoblast differentiation and survival [Globus et al., 1998].

Finally, among the down-regulated genes involved in the growth factor activity molecular functions we observed the *Wisp2* gene, also known as *Connective tissue growth factor like* (*Ctgf-l*) and belonging to the same family of CTGF. This factor is highly expressed in osteoblasts forming bone, and promotes osteoblast adhesion [Kumar et al., 1999].

GENE ONTOLOGY TERMS CLASSIFICATION OF THE UP-REGULATED GENES

The bioinformatics analysis also revealed that some of the up-regulated genes were involved in vivo in important biological processes, such as programmed cell death, response to stress, and selected growth factor activity (Table IV). Among the latter, there is IL-6, whose role in bone homeostasis has been described above. Interestingly, none of the other up-regulated genes could be readily associated with bone metabolism.

COMPARISON OF MICROGRAVITY GENE PROFILING DATA

A recent article published by Xing et al. [2005] identified, by similar microarray analysis using the Agilent® platform, a subset of genes that are significantly modulated by mechanical loading. Starting from these results, and using less stringent conditions (i.e., $P \leq 0.1$; cut-off <0.75 and >1.5), we compared our microarray data to their mechanical loading regulated genes and, among 70 genes, we found 20 common genes that, consistently, changed in opposite directions in the two sets of arrays. Interestingly, this list includes genes coding for ECM protein constituents, such as *Ogn*, *Col8a1* (*Procollagen, type VIII,* α1), *Col14a1* (*Procollagen, type XIV,* α1), *Nid1* (*Nidogen 1*), *Col5a1* (*Procollagen, type V,* α1). Another common gene found was *Pcolc* (*Procollagen C-proteinase enhancer protein*) which enhances the activity of Procollagen C proteinases (pCPs), also known as BMP-1, to cleave type I and III procollagen C propeptides, thus allowing collagen fiber assembling [Kessler and Adar, 1989; Kessler et al., 1996].

We next matched our microgravity genes with gene profiling results obtained by the Patel's group [2007], who performed microarray analysis on 2T3 preosteoblastic cells exposed for 3 days to modeled microgravity using the RWV system. This analysis was performed by the Affymetrix® microarray platform. Among 56

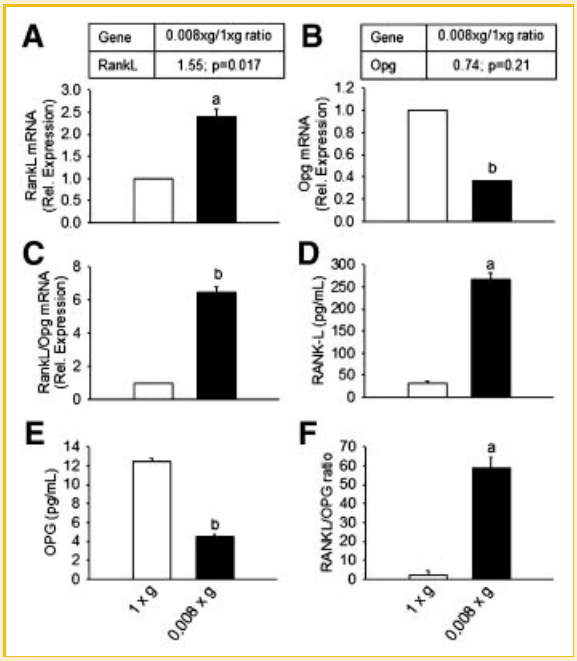

Fig. 6. Effect of modeled microgravity on RANKL and OPG. Primary osteoblasts were grown at unit gravity (1*g*) or under 0.008*g* modeled microgravity for 5 days as described in Figure 1A. Cells were collected, the RNA extracted, and reverse-transcribed. cDNAs were subjected to comparative real-time PCR using primer pairs and conditions specific for (A) *RankL* and (B) *Opg*. Inset tables show the 0.008/1*g* ratio and *P*-value for the indicated genes obtained by microarray analysis. C: Computation of the *RankL/Opg* ratio. Conditioned media were also collected, then the (D) soluble RANKL and (E) OPG were quantified using an ELISA kit, according to the manufacturer's instructions. In (F) the RANKL/OPG protein ratio was determined. Data are the mean ± SEM of three independent experiments ($^{a}P < 0.01$ and $^{b}P < 0.0003$ vs. 1*g*).

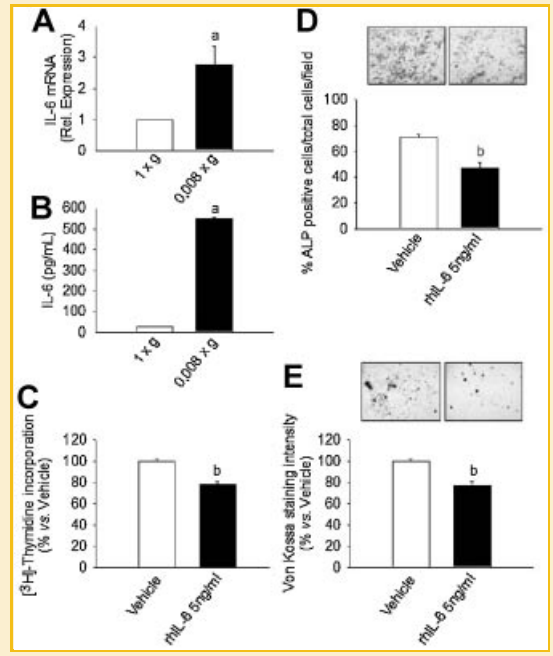

Fig. 7. Effect on IL-6. A,B: Primary osteoblasts were grown at unit gravity (1*g*) or under 0.008*g* modeled microgravity for 5 days as described in Figure 1A. Cells were collected, the RNA extracted, and reverse-transcribed. cDNA was subjected to comparative real-time PCR using primer pairs and conditions specific for (A) *IL-6*. Conditioned media were also collected, and (B) IL-6 quantified using an ELISA kit according to the manufacturer's instructions. C: Primary osteoblasts were cultured in standard conditions, in 24-well plates in the presence of vehicle or 5 ng/ml of recombinant human IL-6 (rhIL-6). Cells were incubated with 2 μCi/ml ^{3}H-thymidine for 24 h, then the radioactivity incorporated was measured in a β counter. D: Primary osteoblasts were treated for 5 days with vehicle or 5 ng/ml of rhIL-6. Cells were then fixed and stained for ALP histochemical detection (upper panels). The percent of ALP-positive cells relative to total number of cells per field was computed (lower panel). E: Primary osteoblasts were treated as described in C for 3 weeks in the presence of ascorbic acid and β-glycerophosphate to favor mineralization. Cells were then fixed and mineralized nodules were detected by the von Kossa staining (upper panels). Graph (lower panel) shows quantitative determination of mineralized nodules performed by densitometric analysis. Data are the mean ± SEM of three independent experiments ($^{a}P < 0.05$ vs. 1*g* and $^{b}P < 0.005$ vs. vehicle). Results in (A) are normalized versus the house-keeping gene *Gapdh*.

genes, 15 were also regulated in our system. These include the matrix proteins *Ogn*, *Col11a1* (*Procollagen*, *type XI*, α1), *Omd* as well as genes regulating osteoblast differentiation, such as *Sfrp2* and *Wisp2*.

Finally, by comparing all three microarray data above mentioned, we identified 10 genes which are commonly down-regulated under microgravity conditions (our data and Patel's results) and up-regulated by the loading condition (Xing's data), as described in Table V. We propose that this list could represent the most reliable "osteoblast mechanoresponsive gene signature."

DISCUSSION

Among the several physiological changes observed in humans exposed to weightlessness, skeletal alterations seem to be particularly serious, leading to bone loss and negative calcium balance [Caillot-Augusseau et al., 1998, 2000; Smith et al., 2005]. In the most severe conditions of weightlessness, there is an approximately 2% decrease in bone mineral density in only 1 month [Collet et al., 1997]. Indeed, astronauts subjected to long-term spaceflights can lose as much bone mass in the proximal femur in 1 month as postmenopausal women on earth lose in 1 year [Bikle et al., 2003; Cavanagh et al., 2005]. Starting from this evidence, there is a need to investigate the underlying molecular mechanisms, in order to prevent or cure bone loss due to weightlessness or, more in general, to unloading conditions.

In this study we identified 133 genes that, in a large-scale microarray analysis performed with the Agilent® platform, are regulated in mouse primary osteoblasts subjected to modeled microgravity (0.008*g*) using the NASA-developed RWV bioreactor. To achieve this result, we decided to use stringent cut-off conditions for the selection of what we named up- and down-regulated genes. The up-regulated genes had a mean fold increase major than 2 and a *P*-value obtained from the *t*-test analysis minor than 0.05, while the down-regulated genes had a mean fold increase minor than 0.5 and a *P*-value obtained from the *t*-test analysis minor than 0.05. Although we are aware that the gene microarray does not measure

TABLE III. List of the Down-Regulated Genes Clustered According to the Molecular Function in Which They Are Involved (GOTM Platform)

Systematic name	Gene symbol	Gene name	Fold Δ	*P*-value	Function
Down-regulated genes involved in the "extracellular matrix components" molecular function					
NM_007739	Col8a1	Procollagen, type VIII, alpha 1	0.24	0.0002	Phosphate transport, cell adhesion, eye morphogen
NM_010217	Ctgf	Connective tissue growth factor	0.28	0.026	Integrin binding, heparin binding, insulin-like growth factor binding, cell matrix adhesion, cell migration
NM_007993	Fbn1	Fibrillin 1	0.45	0.055	Calcium ion binding, chitin metabolism
NM_181277	Col14a1	Procollagen, type XIV, alpha 1	0.37	0.007	Phosphate transport, cell adhesion
NM_025711	Aspn	Asporin	0.15	0.021	Transferase activity, porin activity
NM_008760	Ogn	Osteoglycin	0.21	0.012	Growth factor activity, transferase activity
NM_012050	Omd	Osteomodulin	0.36	0.027	Transferase activity, cell adhesion
NM_010917	Nid1	Nidogen 1	0.39	0.004	Calcium ion binding, protein binding, cell adhesion
NM_029568	Mfap4	Microfibrillar-associated protein 4	0.50	0.008	Calcium ion binding, cell adhesion, protein binding
NM_011821	Gpc6	Glypican 6	0.49	0.042	GPI anchor binding
Down-regulated genes involved in the "glycosaminoglycans or heparin-binding" molecular function					
NM_010217	Ctgf	Connective tissue growth factor	0.28	0.026	Integrin binding, heparin binding, insulin-like growth factor binding, cell matrix adhesion, cell migration
NM_010233	Fn1	Fibronectin 1	0.35	0.021	Protease activator activity, cell–substrate junction assembly, cell–matrix adhesion, cell morphogenesis
NM_015784	Postn	Periostin, osteoblast-specific factor	0.38	0.007	Cell adhesion, extracellular matrix organization
NM_011581	Thbs2	Thrombospondin 2	0.41	0.110	Calcium ion binding, cell adhesion
Down-regulated genes involved in the "growth factor activity" molecular function					
NM_008760	Ogn	Osteoglycin	0.21	0.012	Growth factor activity, transferase activity
NM_011313	S100a6	S100 calcium-binding protein A6 (calcyclin)	0.22	0.033	Calcium, zinc ion-binding, cell proliferation
NM_010514	Igf2	Insulin-like growth factor 2	0.40	0.005	Cell proliferation, organ morphogenesis
NM_009131	Clec11a	C-type lectin domain family 11, member a	0.41	0.010	Positive regulator of cell proliferation
NM_016873	Wisp2	WNT1 inducible signaling pathway protein 2	0.42	0.050	Calcium ion binding, insulin-like growth factor binding, phospholipase A2 activity

the absolute quantity of transcripts, we are confident that these results are reliable because the real-time RT-PCR analysis validated the regulations identified in the microarray experiments for all the analyzed genes.

Some of these genes could be easily associated with bone metabolism, such as the master gene *Runx2*, which is in agreement with previous reports [Nakamura et al., 2003; Zayzafoon et al., 2004; Pardo et al., 2005]. Other genes involved in osteoblast differentiation were *Sfrp2* and *Wisp2*, which belong to the wnt pathway. Our gene profiling results also evidenced a significant decrease of ECM components with glycosaminoglycan/heparin-binding activity, such as *Omd*, *Ogn*, *Fn1*, *Pstn*, and *Ctgf*, along with several procollagen genes. Furthermore, we found a decrease of *Cdh-11*, also known as osteoblast cadherin, a Ca^{2+}-dependent homophilic cell adhesion molecule that is expressed mainly in osteoblasts. Indeed, a recent study demonstrated that cell–cell interaction mediated by CDH11 directly regulates the differentiation of mesenchymal cells into cells of the osteo- and chondro-lineages

TABLE IV. List of the Up-Regulated Genes Clustered According to the Biological or Molecular Function in Which They Are Involved (GOTM Platform)

Systematic name	Gene symbol	Gene name	Fold Δ	*P*-value	Function
Up-regulated genes involved in the "programmed cell death" biological process					
NM_031168	Il6	Interleukin 6	4.44	0.048	Cytokine activity, growth factor activity, immune response
NM_008303	Hspe1	Heat shock protein 1 (chaperonin 10)	2.33	0.004	Chaperonin binding, ATP binding
NM_007808	Cycs	Cytochrome c, somatic	2.10	0.00009	Electron carrier activity, metal ion binding
NM_009344	Phlda1	Pleckstrin homology-like domain, family A, 1	2.24	0.048	FasL biosynthesis, apoptosis
Up-regulated genes involved in the "response to stress" biological process					
NM_031168	Il6	Interleukin 6	4.44	0.0479	Cytokine activity, growth factor activity, immune response
NM_007453	Prdx6	Peroxiredoxin 6	2.22	0.007	Antioxidant activity, hydrolase, oxidoreductase, and peroxidase activities
NM_008706	Nqo1	NAD(P)H dehydrogenase, quinone 1	6.38	0.005	Oxidoreductase activity, electron transport
NM_011171	Procr	Protein C receptor, endothelial	2.81	0.041	Protein C-terminus binding, neg. regul. of coagulation
NM_011315	Saa3	Serum amyloid A 3	2.70	0.020	Lipid transporter activity
NM_013671	Sod2	Superoxide dismutase 2, mitochondrial	2.65	0.002	Oxidoreductase activity, metal ion binding
NM_029688	Srxn1	Sulfiredoxin 1 homolog (*S. cerevisiae*)	2.19	0.003	Antioxidant activity, ATP binding, nucleotide binding
NM_030704	Hspb8	Heat shock 27 kDa protein 8	2.10	0.002	Serine/threonine kinase activity, protein folding
Up-regulated genes involved in "the growth factor activity" molecular function					
NM_031168	Il6	Interleukin 6	4.44	0.048	Cytokine activity, growth factor activity, immune response
NM_008380	Inhba	Inhibin beta-A	2.53	0.0006	Hormone activity
NM_013609	Ngfb	Nerve growth factor, beta	2.51	0.032	Regulation of neuron differentiation
NM_008176	Cxcl1	Chemokine (C-X-C motif) ligand 1	2.20	0.0004	Inflammatory response, immune response, cytokine activity

TABLE V. List of the Common Regulated Genes Among Our Data (MCG), Patel's Microgravity Results (35) (MCG-P) and Xing's Mechanical Loading Results (20) (Loading) (Cut-Off <0.75; $P \leq 0.1$)

Systematic name	Gene symbol	Gene name	Fold Δ, MCG	*P*-value, MCG	Fold Δ, MCG-P	*P*-value, MCG-P	Fold Δ, loading	*P*-value, loading
NM_008760	Ogn	Osteoglycin	0.21	0.012	0.23	0.03	2.47	0.004
NM_008809	Pdgfrb	Platelet-derived growth factor receptor, beta polypeptide	0.37	0.029	0.74	0.25	1.97	0.008
NM_008409	Itm2a	Integral membrane protein 2A	0.37	0.005	0.31	0.17	2.85	0.003
NM_009128	Scd2	Stearoyl-coenzyme A desaturase 2	0.47	0.007	0.4	0.28	2.56	0.0025
NM_007792	Csrp2	Cysteine and glycine-rich protein 2	0.48	0.026	0.65	<0.05	4.12	0.001
NM_008788	Pcolc	Procollagen C-proteinase enhancer protein	0.52	0.0006	0.56	<0.01	2.15	0.0086
NM_015734	Col5a1	Procollagen, type V, alpha 1	0.54	0.07	0.56	0.06	1.97	0.0011
NM_026840	Pdgfrl	Platelet-derived growth factor receptor like	0.68	0.08	0.45	<0.005	2.18	0.0026
NM_009037	Rcn1	Reticulocalbin1	0.69	0.005	0.69	<0.05	2.31	0.004
NM_011175	Lgmn	Legumain	0.73	0.05	0.64	0.25	3.25	0.003

[Kii et al., 2004]. *Asp*, another gene modulated by microgravity, is an ECM protein that belongs to the SLRP family of proteins. Its biological role has been unclear, but recent genetic studies have demonstrated association between asporin and various bone and joint diseases, including osteoarthritis, rheumatoid arthritis, and lumbar disc disease [Ikegawa, 2008]. Altogether these data are consistent with the ability of modeled microgravity to decrease osteoblast differentiation and function, with a consequent impairment of bone matrix production.

Interestingly, the most regulated genes were *Penk1* (down) and *Lcn2* (up). The former encodes for four copies of met-enkephalin, two copies of met-enkephalin extended sequences, and one copy of leu-enkephalin, which are endogenous opioid neuropeptides involved in the behavioral response to stimuli [Litt et al., 1988]. LCN2, also known as NGAL, is a protein associated with neutrophil gelatinase [Kjeldsen et al., 1993], which is believed to bind small lipophilic substances, such as bacteria-derived lipopolysaccharide (LPS) and formylpeptides, thus functioning as a modulator of inflammation. LCN2 is also activated by IL-3 withdrawal-mediated apoptosis [Devireddy et al., 2001]. Despite the robust regulation of these genes under our microgravity conditions, to the best of our knowledge they have not been associated so far with bone metabolism, and we are now taking the challenge to investigate their role in this context. Among the genes not obviously related to bone, we also found *Tnmd*, coding for an angiogenesis inhibitor found in dense connective tissues, including tendons and ligaments [Shukunami et al., 2008], and *Nqo1*, coding for a cytosolic protein that, together with NQO2, catalyzes metabolic reduction of quinones and its derivatives to protect cells against redox cycling [Iskander and Jaiswal, 2005].

We have previously shown that osteoblasts subjected to modeled microgravity for a shorter time (24 h) were capable of indirectly stimulating osteoclast formation and activity by regulating secretion of crucial factors such as RANKL and OPG by osteoblasts [Rucci et al., 2007]. The gene profiling results presented here evidenced again an increase of RANKL and a decrease of OPG, thus strengthening the role of the RANKL/OPG pathway in simulated microgravity-induced osteoclastogenesis. Interestingly, in our former short-term study [Rucci et al., 2007], we did not find significant changes of genes associated with osteoblast differentiation and function. Therefore, we believe that the two reports together reveal that osteoblast-induced bone resorption is the earliest event triggered by modeled microgravity, followed at a later stage by impairment of osteoblast function. These observations may have a translational impact because it could be hypothesized that antiresorptive agents could suffice to block bone loss in individuals subjected to short-term spaceflights, while anabolic agents may be necessary to balance bone loss induced by long-term permanence in space.

Interestingly, among the up-regulated genes, there was also IL-6, whose osteoclast-stimulating role has been well recognized [Kudo et al., 2003; Liu et al., 2006; Smolen and Maini, 2006]. However, its effect is likely to be subjected in vivo to a variety of other conditions, including coupling with the osteoblast activity in the remodeling process [Sims et al., 2004; De Benedetti et al., 2006]. Indeed, our results underline a potential role of IL-6 in unloading conditions, which, along with the RANKL/OPG axis, could contribute to the enhancement of osteoclastogenesis and bone resorption. In addition, it could cause impairment of osteoblast proliferation, differentiation, and function acting as an autocrine negative regulator, as we also demonstrated in this study. These findings could have an important translational meaning for therapeutic applications, as anti-IL-6 agents are currently in clinical trials for inflammatory diseases [Yokota et al., 2008].

Finally, we compared our gene profiling results with microarray data from two independent groups: the group of Xing et al. [2005] who performed gene profiling on mechanically loaded tibiae in a mouse model, and the group of Patel et al. [2007] who worked on preosteoblastic 2T3 cells under simulated microgravity using the RWV bioreactor. Matching these results we identified a selected cluster of genes common to the three sets, whose regulation was consistently in opposite direction when loading and unloading conditions were compared. This set is quite heterogeneous and ranges from ECM constituents (*Ogn*, *Col5a1*) and genes involved in collagen fiber assembly (*Pcolc*) to growth factor receptors (*Pdgfrb*, *Pdgfrl*) and genes coding for enzymes. These latter include *Scd2* (*Stearoyl-Coenzyme A desaturase 2*) which is important in lipid synthesis in early development [Miyazaki et al., 2005] and *Lgmn* (*Legumain*), encoding a cysteine protease that hydrolyzes asparaginyl bonds and has a pivotal role in the endosomal/lysosomal degradation system [Shirahama-Noda et al., 2003]. Interestingly, we also found *Itm2a* (*integral membrane protein 2a*) a gene that has

been shown to be a marker of chondrogenic/osteoblastic cells in bone formation [Tuckermann et al., 2000]. Since alteration of these genes is associated with the mechanoresponsive ability of osteoblasts, we believe that they may identify a reliable ''osteoblast mechanoresponsive gene signature.'' It will be interesting to recognize whether they may also represent a subset of genes that may predict susceptibility to osteoporosis or to other pathological conditions.

In conclusion, our global analysis identified a subset of significantly regulated genes in mouse primary osteoblast cultures subjected to modeled microgravity. Some of these genes can readily be associated with bone metabolism and their regulation is consistent with the condition of unloading that we mimicked using the RWV. Among them, genes involved in osteoblast differentiation/function and in osteoblast–osteoclast cross-talk appear to play prominent roles. Interestingly, our data also showed the regulation of some genes whose involvement in bone homeostasis had not yet been recognized. These data could contribute to a better understanding of the mechanisms underlying bone mass regulation and to the identification of new targetable molecules, to prevent and/or cure bone loss in individuals subjected to unloading conditions or affected by metabolic bone diseases.

ACKNOWLEDGMENTS

We thank Dr. Rita Di Massimo for her assistance in editing this manuscript. Agenzia Spaziale Italiana (ASI) to A. Teti (Grant number: I/007/06/0).

REFERENCES

Arnott JA, Nuglozeh E, Rico MC, Arango-Hisijara I, Odgren PR, Safadi FF, Popoff SN. 2007. Connective tissue growth factor (CTGF/CCN2) is a downstream mediator for TGF-beta1-induced extracellular matrix production in osteoblasts. J Cell Physiol 210:843–852.

Balint E, Lapointe D, Drissi H, van der Meijden C, Young DW, van Wijnen AJ, Stein JL, Stein GS, Lian JB. 2003. Phenotype discovery by gene expression profiling: Mapping of biological processes linked to BMP-2-mediated osteoblast differentiation. J Cell Biochem 89:401–426.

Bikle DD, Halloran BP. 1999. The response of bone to unloading. J Bone Miner Metab 17:233–244.

Bikle DD, Sakata T, Halloran BP. 2003. The impact of skeletal unloading on bone formation. Gravit Space Biol Bull 16:45–54.

Caillot-Augusseau A, Lafage-Proust MH, Soler C, Pernod J, Dubois F, Alexandre C. 1998. Bone formation and resorption biological markers in cosmonauts during and after a 180 day space flight (Euromir 95). Clin Chem 44:578–585.

Caillot-Augusseau A, Vico L, Heer M, Voroviev D, Souberbille JC, Zitterman A, Alexandre C, Lafage-Proust MH. 2000. Space flight is associated with rapid decrease of undercarboxylated osteocalcin and increase of markers of bone resorption without changes in their circadian variations: Observations in two cosmonauts. Clin Chem 46:1136–1143.

Carmeliet G, Bouillon R. 1999. The effect of microgravity on morphology and gene expression of osteoblasts in vitro. FASEB J 13:S129–S134.

Cavanagh PR, Licata AA, Rice AJ. 2005. Exercise and pharmacological countermeasures for bone loss during long-duration space flight. Gravit Space Biol Bull 18:39–58.

Collet P, Uebelhart D, Vico L, Moro L, Hartmann D, Roth M, Alexandre C. 1997. Effect of 1- and 6-month spaceflight on bone mass and biochemistry in two humans. Bone 20:547–551.

De Benedetti F, Rucci N, Del Fattore A, Peruzzi B, Paro R, Longo M, Vivarelli M, Muratori F, Berni S, Ballanti P, Ferrari S, Teti A. 2006. Impaired skeletal development in interleukin-6-transgenic mice: A model for the impact of chronic inflammation on the growing skeletal system. Arthritis Rheum 54:3551–3563.

Devireddy LR, Teodoro JC, Richard FA, Green MR. 2001. Induction of apoptosis by a secreted lipocalin that is transcriptionally regulated by IL-3 deprivation. Science 293:829–834.

Duray PH, Hatfill SJ, Pellis NR. 1997. Tissue culture in microgravity. Sci Med May/June: 45–55.

Globus RK, Doty SB, Lull JC, Holmuhamedov E, Humphries MJ, Damsky CH. 1998. Fibronectin is a survival factor for differentiated osteoblasts. J Cell Sci 111:1385–1393.

Horiuchi K, Amizuka N, Takeshita S, Takamatsu H, Katsuura M, Ozawa H, Toyma Y, Bonewald LF, Kudo A. 1999. Identification and characterization of a novel protein, periostin, with restricted expression to periosteum and periodontal ligament and increased expression by transforming growth factor beta. J Bone Miner Res 14:1239–1249.

Hsieh YF, Robling AG, Ambrosius WT, Burr DB, Turner CH. 2001. Mechanical loading of diaphyseal bone in vivo: The strain threshold for an osteogenic response varies with location. J Bone Miner Res 16:2291–2297.

Ikegawa S. 2008. Expression, regulation and function of asporin, a susceptibility gene in common bone and joint diseases. Curr Med Chem 15:724–728.

Iskander K, Jaiswal AK. 2005. Quinone oxidoreductases in protection against myelogenous hyperplasia and benzene toxicity. Chem Biol Interact 153–154:147–157.

Kessler E, Adar R. 1989. Type I procollagen C-proteinase from mouse fibroblasts. Purification and demonstration of a 55-kDa enhancer glycoprotein. Eur J Biochem 186:115–121.

Kessler E, Takahara K, Biniaminov L, Brusel M, Greenspan DS. 1996. Bone morphogenetic protein-1: The type I procollagen C-proteinase. Science 271:360–362.

Kii I, Amizuka N, Shimomura J, Saga Y, Kudo A. 2004. Cell-cell interaction mediated by cadherin-11 directly regulates the differentiation of mesenchymal cells into the cells of the osteo-lineage and the chondro-lineage. J Bone Miner Res 19:1840–1849.

Kjeldsen L, Johnsen AH, Sengelov H, Borregaard N. 1993. Isolation and primary structure of NGAL, a novel protein associated with human neutrophil gelatinase. J Biol Chem 268:10425–10432.

Kouadjo KE, Nishida Y, Cadrin-Girard JF, Yoshioka M, St-Amand J. 2007. Housekeeping and tissue-specific genes in mouse tissues. BMC Genomics 8:127.

Kudo O, Sabokbar A, Pocock A, Itonaga I, Fujikawa Y, Athanasou NA. 2003. Interleukin-6 and interleukin-11 support human osteoclast formation by a RANKL-independent mechanism. Bone 32:1–7.

Kumar S, Hand AT, Connor JR, Dodds RA, Ryan PJ, Trill JJ, Fisher SM, Nuttall ME, Lipshutz DB, Zou C, Hwang SM, Votta BJ, James IE, Rieman DJ, Gowen M, Lee JC. 1999. Identification and cloning of a connective tissue growth factor-like cDNA from human osteoblasts encoding a novel regulator of osteoblasts functions. J Biol Chem 274:17123–17131.

Litt M, Buroker NE, Kondoleon SK, Liston D, Douglass J, Sheehy R, Magenis RE. 1988. Chromosomal localization of the human proenkephalin and prodynorphin genes. Am J Human Genet 42:327–334.

Liu XH, Kirschenbaum A, Yao S, Levine AC. 2006. Interactive effect of interleukin-6 and prostaglandin E2 on osteoclastogenesis via the OPG/RANKL/RANK system. Ann NY Acad Sci 1068:225–233.

Marzia M, Sims NA, Voit S, Migliaccio S, Taranta A, Bernardini S, Faraggiana T, Yoneda T, Mundy GR, Boyce BF, Baron R, Teti A. 2000. Decreased c-Src

expression enhances osteoblast differentiation and bone formation. J Cell Biol 151:311–320.

Miyazaki M, Dobrzyn A, Elias PM, Ntambi JM. 2005. Stearoyl-CoA desaturase-2 gene expression is required for lipid synthesis during early skin and liver development. Proc Natl Acad Sci USA 102:12501–12506.

Nakamura H, Kumei Y, Morita S, Shimokawa H, Ohya K, Shinomiya K. 2003. Suppression of osteoblastic phenotypes and modulation of pro- and anti-apoptotic features in normal human osteoblastic cells under a vector-averaged gravity condition. J Med Dent Sci 50:167–176.

Pardo SJ, Patel MJ, Sykes MC, Platt MO, Boyd NL, Sorescu GP, Xu M, van Loon JJ, Wang MD, Jo H. 2005. Simulated microgravity using the random positioning machine inhibits differentiation and alters gene expression profiles of 2T3 preosteoblasts. Am J Physiol Cell Physiol 288:C1211–C1221.

Patel MJ, Liu W, Sykes MC, Ward NE, Risin SA, Risin D, Jo H. 2007. Identification of mechanosensitive genes in osteoblasts by comparative microarray studies using the rotating wall vessel and the random positioning machine. J Cell Biochem 101:587–599.

Ramstad VE, Franzèn A, Heinegård D, Wendel M, Reinholt FP. 2003. Ultrastructural distribution of osteoadherin in rat bone shows a pattern similar to that of bone sialoprotein. Calcif Tissue Int 72:57–64.

Rehn AP, Chalk AM, Wendel M. 2006. Differential regulation of osteoadherin (OSAD) by TGF-beta1 and BMP2. Biochem Biophys Res Commun 349:1057–1064.

Robling AG, Burr DB, Turner CH. 2001. Recovery periods restore mechanosensitivity to dynamically loaded bone. J Exp Biol 204:3389–3399.

Rucci N, Migliaccio S, Zani BM, Taranta A, Teti A. 2002. Characterization of the osteoblast-like cell phenotype under microgravity conditions in the NASA-approved rotating wall bioreactor (RWV). J Cell Biochem 85:167–179.

Rucci N, Rufo A, Alamanou M, Teti A. 2007. Modeled microgravity stimulates osteoclastogenesis and bone resorption by increasing osteoblast RANKL/OPG ratio. J Cell Biochem 100:464–473.

Shirahama-Noda K, Yamamoto A, Sugihara K, Hashimoto N, Asano M, Nishimura M, Hara-Nishimura I. 2003. Biosynthetic processing of cathepsins and lysosomial degradation are abolished in asparaginyl endopeptidase-deficient mice. J Biol Chem 278:33194–33199.

Shukunami C, Takimoto A, Miura S, Nishizaki Y, Hiraki Y. 2008. Chondromodulin-I and tenomodulin are differentially expressed in the avascular mesenchyme during mouse and chick development. Cell Tissue Res 332:111–122.

Sims NA, Jenkins BJ, Quinn JM, Nakamura A, Glatt M, Gillespie MT, Ernst M, Martin TJ. 2004. Glycoprotein 130 regulates bone turnover and bone size by distinct downstream signalling pathways. J Clin Invest 113:379–389.

Smith SM, Wastney ME, O'Brien KO, Morukov BV, Larina IM, Abrams SA, Davis-Street JE, Oganov V, Shackelford LC. 2005. Bone markers, calcium metabolism, and calcium kinetics during extended-duration space flight of the mir space station. J Bone Miner Res 20:208–218.

Smolen JS, Maini RN. 2006. Interleukin-6: A new therapeutic target. Arthritis Res Ther 8:S5.

Sommarin Y, Wendel M, Shen Z, Hellman U, Heinegård D. 1998. Osteoadherin, a cell-binding keratan sulfate proteoglycan in bone, belongs to the family of leucine-rich repeat proteins of the extracellular matrix. J Biol Chem 273:16723–16729.

Sonnenfeld G, Butel JS, Shearer WT. 2003. Effects of the space flight environment on the immune system. Rev Environ Health 18:1–17.

Tasheva ES, Koester A, Paulsen AQ, Garrett AS, Boyle DL, Davidson HJ, Song M, Fox N, Conrad GW. 2002. Mimecan/osteglycin-deficient mice have collagen fibril abnormalities. Mol Vis 8:407–415.

Tesch PA, Berg HE, Bring D, Evans HJ, LeBlanc AD. 2005. Effects of 17-day spaceflight on knee extensor muscle function and size. Eur J Appl Physiol 93:463–468.

Tilton FE, Degioanni JJ, Schneider VS. 1980. Long term follow-up of Skylab bone demineralisation. Mol Biol Cell 15:625–636.

Tuckermann JP, Pittois K, Partridge NC, Merregaert J, Angel P. 2000. Collagenase-3 (MMP-13) and integral membrane protein 2a (Itm2a) are marker genes of chondrogenic/osteoblastic cells in bone formation: sequential temporal, and spatial expression of Itm2a, alkaline phosphatase, MMP-13, and osteocalcin in the mouse. J Bone Miner Res 15:1257–1265.

Tuday EC, Meck JV, Nyhan D, Shoukas AA, Berkowitz DE. 2007. Microgravity-induced changes in aortic stiffness and their role in orthostatic intolerance. J Appl Physiol 102:853–858.

Van Loon JJWA, Bervoets DJ, Burger EH, Dieudonne SC, Hagen JW, Semeins CM, Doulabi BZ, Veldhuijzen JP. 1995. Decreased mineralization and increased calcium release in isolated fetal mouse long bones under near weightlessness. J Bone Miner Res 10:550–557.

Xing W, Baylink D, Kesavan C, Hu Y, Kapoor S, Chadwick RB, Mohan S. 2005. Global gene expression analysis in the bones reveals involvement of several novel genes and pathways in mediating an anabolic response of mechanical loading in mice. J Cell Biochem 96:1049–1060.

Yokota S, Imagawa T, Mori M, Miyamae T, Aihara Y, Iwata N, Umbeyashi H, Murata T, Miyoshi M, Tomiita M, Nashimoto N, Kishimoto T. 2008. Efficacy and safety of tocilizumab in patients with systemic-onset juvenile idiopathic arthritis: A randomised, double-blind, placebo-controlled, withdrawal phase III trial. Lancet 371:998–1006.

Zayzafoon M, Gathings WE, McDonald JM. 2004. Modeled microgravity inhibits osteogenic differentiation of human mesenchymal stem cells and increases adipogenesis. Endocrinology 145:2421–2432.

Zhang B, Schmoyer D, Kirov S, Snoddy J. 2004. GOTree Machine (GOTM): A web-based platform for interpreting sets of interesting genes using Gene Ontology hierarchies. BMC Bioinformatics 5:16.